Electronic Supplementary Material (ESI) for Journal of Materials Chemistry A.

Supporting Information

Janus Evaporator with Low Tortuosity for Long-Term Solar Desalination

Rong Hu[(a) †], *Junqi Zhang*[(a) ‡], *Yudi Kuang*[(a) ‡], *Kebing Wang*[†], *Xiaoying Cai*[†], *Zhiqiang Fang*[‡], *Wenqi Huang*[*†], *Gang Chen*[*‡], *and Zhongxing Wang*[*†]

[a] These authors contributed equally to this work.

[†]Department of Anesthesiology, Sun Yat-sen University First Affiliated Hospital, Guangzhou 510080, P. R. China

[‡] State Key Laboratory of Pulp and Paper Engineering, South China University of Technology, Guangzhou 510640, P. R. China

[*]Email: doctorwzx@126.com (Z. Wang); papercg@scut.edu.cn (G. Chen) ; huangwenqi86@aliyun.com (W. Huang)

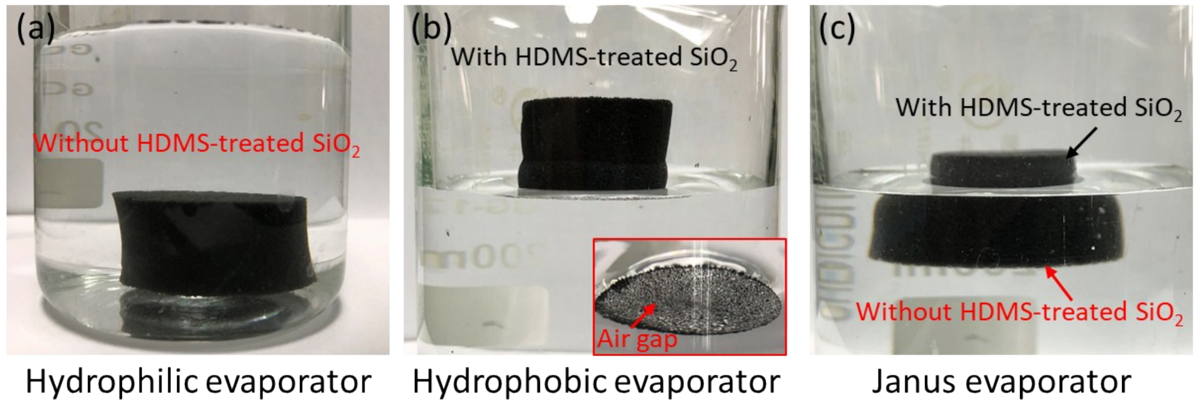

Fig. S1 Photographs illustrating the influence of HDMS-treated SiO_2 coating on the floating property of the evaporators. (a) sunken evaporator without HDMS-treated SiO_2 coating. (b) floating evaporator with all the surface coated with HDMS-treated SiO_2. Inset image showing the nonwetted bottom of the evaporator. (c) half-immersed Janus evaporator with fully wetted water supplying layer and hydrophobic solar absorption layer.

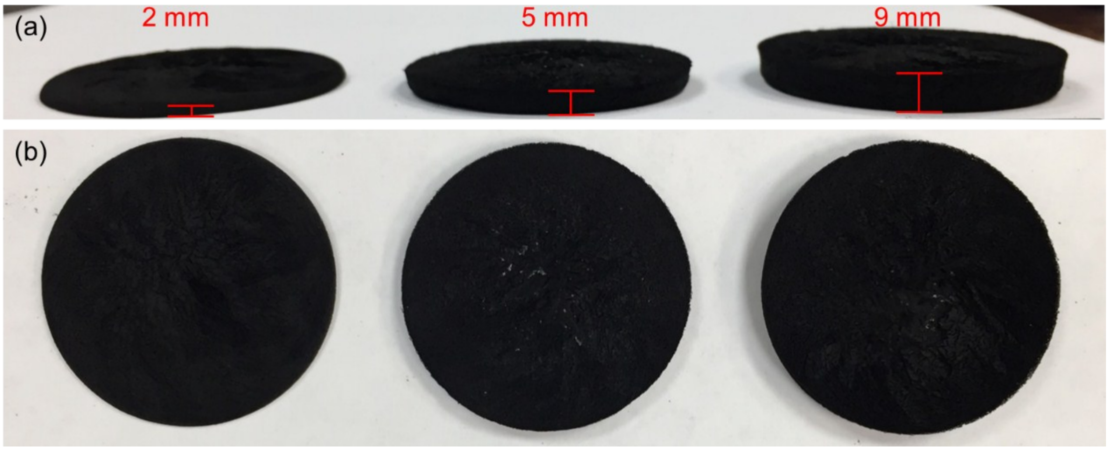

Fig. S2 (a) Side view and (b) top view photographs of the Janus evaporator with different thicknesses.

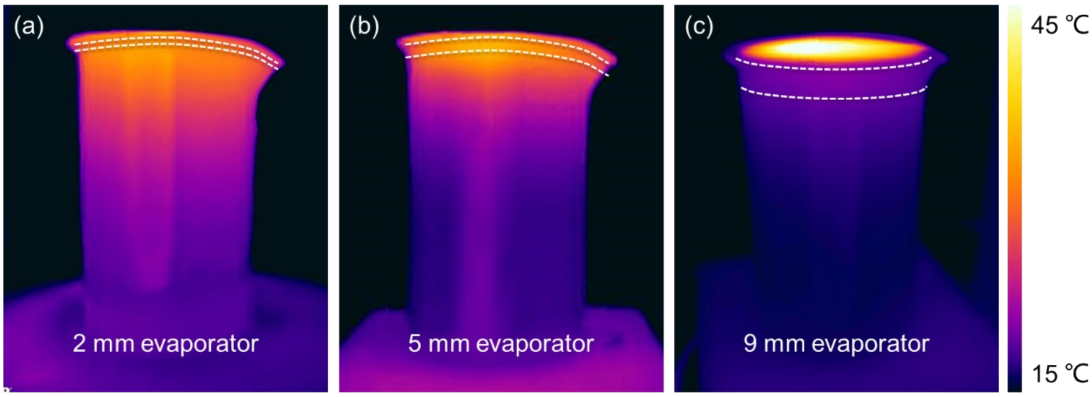

Fig. S3 IR images illustrating the influence of evaporator thickness on the heat localization performance with a solar irradiance of 1-sun.

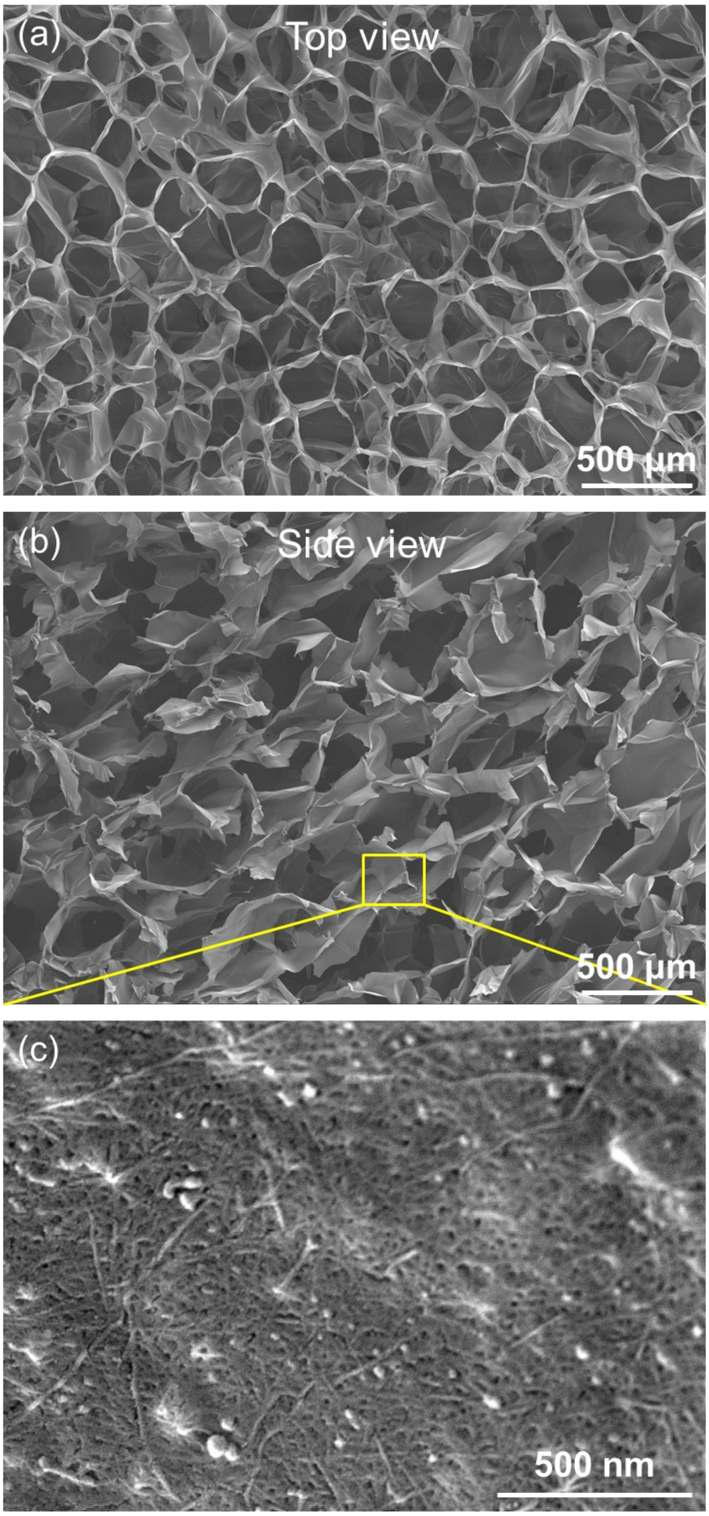

Fig. S4 Morphology characterization of the evaporator with random pore structure prepared by the conventional freezing method: (a) top view and (b) side view SEM images showing the high tortuosity pore structure of the evaporator; (c) magnified image showing the hybrid CNF/CNT network on the wall.

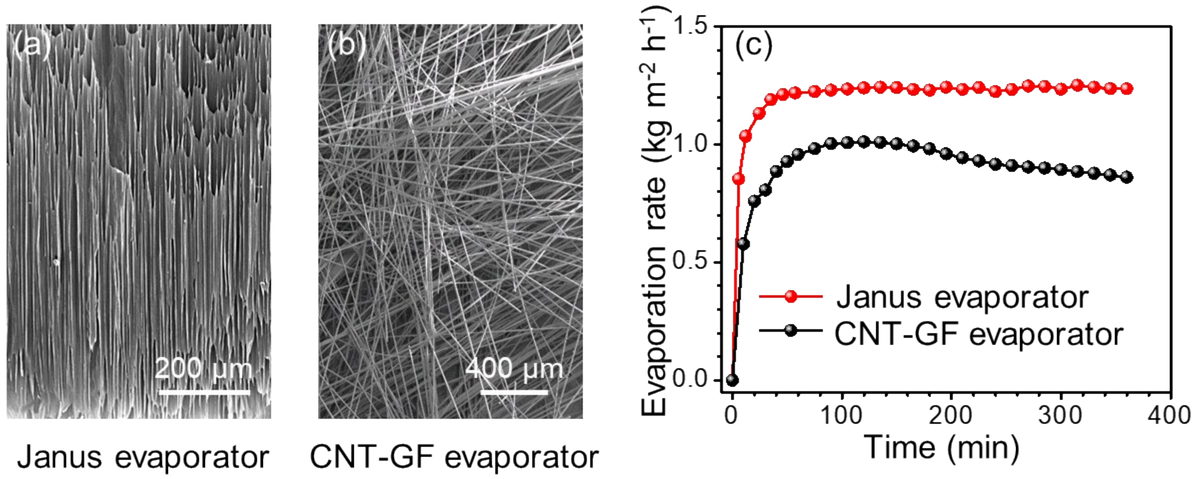

Fig. S5 SEM images showing the different pore structures of (a) the Janus evaporator and (b) the CNT-GF evaporator. (c) time-dependent evaporation rate of the Janus evaporator with low tortuosity pore structure and the CNT-GF evaporator with high tortuosity pore structure.

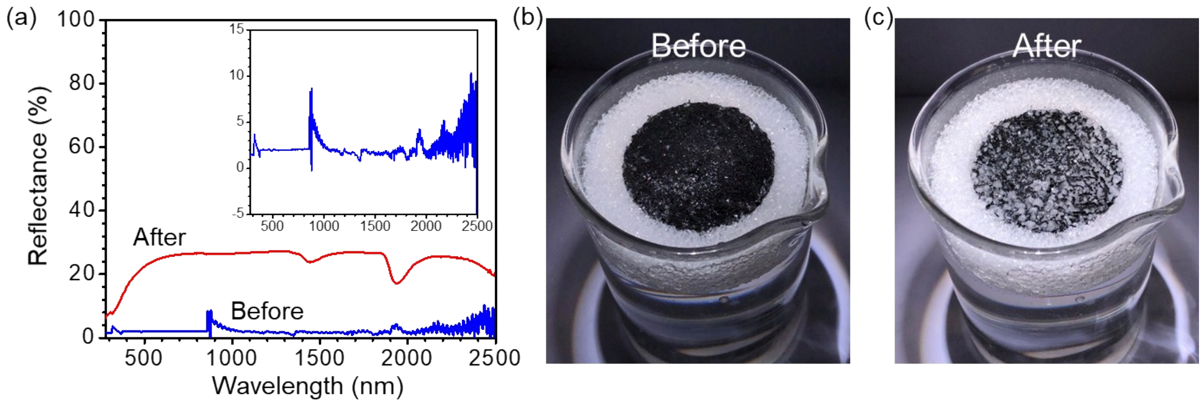

Fig. S6 (a) Reflectance spectrum of the CNF/CNT evaporator before and after testing in 3.5 wt% NaCl solution with a solar irradiance of 1-sun for 6 hours. In set plot is the magnified image of the reflectance spectrum of the evaporator before solar desalination. The deposited salt at the surface of the evaporator significantly increased the light reflection ratio, leading to a deteriorated solar absorption; (b–c) photographs showing the salt deposition issues before and after the solar desalination test.

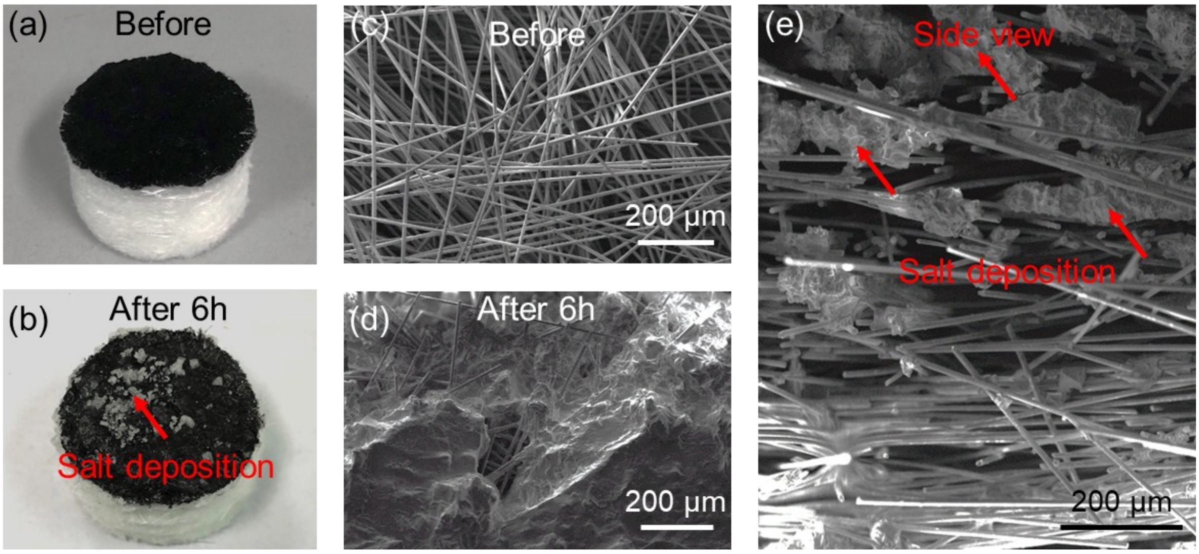

Fig. S7 (a-b) Photographs of the CNT-GF evaporator before and after testing in 3.5 wt% NaCl solution with a solar irradiance of 1-sun for 6 hours. (c-d) Top-view and (e) side-view SEM images illustrating the salt clogging issues of the CNT-GF evaporator after solar desalination test.

Note S1. Irradiation heat calculation of the evaporator with a surface of 43 ^{o}C.

The irradiation loss of the evaporator is calculated according to the Stefan-Boltzmann equation, as expressing,

$$\Phi = \varepsilon A \sigma (T_e^4 - T_i^4)$$

$$Radiation\ loss = \frac{\Phi}{A C_{opt} q_i} = \frac{\varepsilon \sigma (T_e^4 - T_i^4)}{C_{opt} q_i}$$

where Φ represents the heat flux, ε represents the emissivity which is set to be 1 here, A represents the exposed area, σ represents the Stefan-Boltzmann constant which is 5.67×10-8 J m^{-2} s^{-1} K^{-4}, T_i and T_e are the stable surface temperature of the evaporator before (20 ^{o}C) and after (43 ^{o}C) solar irradiation, respectively, C_{opt} represent the optical concentration of the solar which is 1 here, q_i represent the nominal solar illumination (1 kW m^{-2}). Therefore, the thermal irradiation loss of the Janus evaporator with a surface of 43 ^{o}C (1 sun) is calculated to be 10.25%.

Note S2. Salt Excretion Rate of The Evaporator During Solar Desalination

Although the salt in the evaporator can be excreted via two mechanisms, diffusion and advection, we assumed that the salt excretion in our evaporator was mainly occurring by the diffusion mechanism due to the steady state of the bulk solution during solar desalination.

According to Fick's first law of diffusion,

$$F = - D\frac{d\varphi}{dx}$$

where F represents the diffusion flux of salt and D represents the diffusion coefficient of NaCl in water which is 1.99 × 10^{-9} m^2 s^{-1}, $\frac{d\varphi}{dx}$ is the concentration gradient.

As for the Janus evaporator, as shown in Fig. S8, the salt excretion rate $F_{exc.}$ in the evaporator can be expressed as follows:

$$F_{exc.} = D\frac{\varphi_i - \varphi_b}{\tau L}$$

where φ_i and φ_b represent the salt concentration at the evaporation interfaces (where we assume saturation) and the bulk solution (Table S2), respectively; τL represents the length that the salt needs to move from the evaporation interfaces to the bulk solution, τ represents the tortuosity of the evaporator and L represents the projected salt transfer length along the thickness direction of the evaporator.

The salt generation rate $F_{gen.}$ at the evaporation interface is calculated as follows:

$$F_{gen.} = E \times \frac{\varphi_b}{1 - \varphi_b}$$

where E represents the steam generation rate at the evaporation interfaces, which we set to be 1.24 kg m^{-2} s^{-1} for 1-sun.

Therefore, based on mass balance at the solar evaporation interfaces, in order to prevent salt deposition, requiring $F_{gen.} \leq F_{exc.}$, which represents a maximum salt concentration of 11.6 wt% for the 9 mm Janus evaporator (Fig. S9).

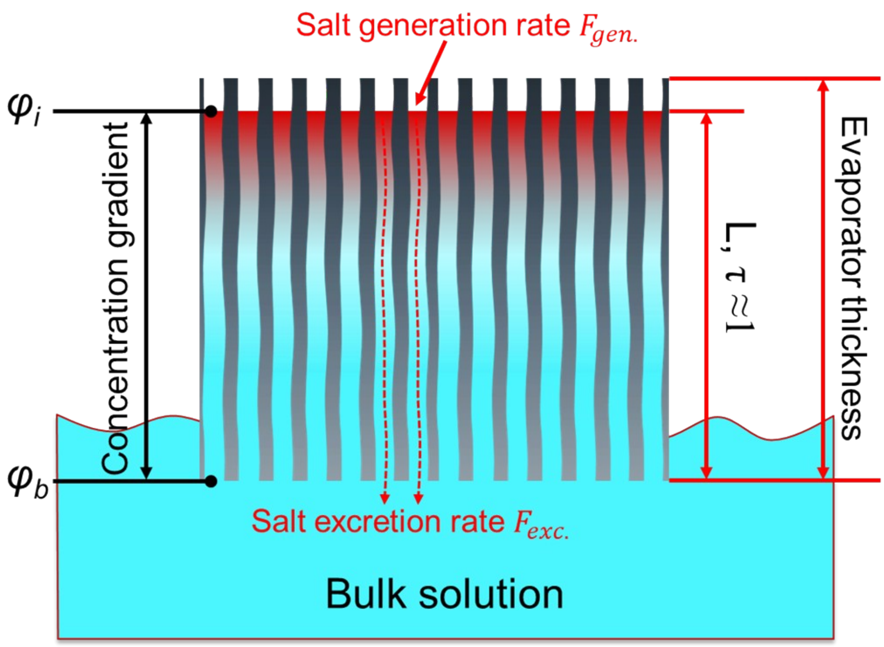

Fig. S8 Schematic showing the structural characteristics of the Janus evaporator during solar desalination.

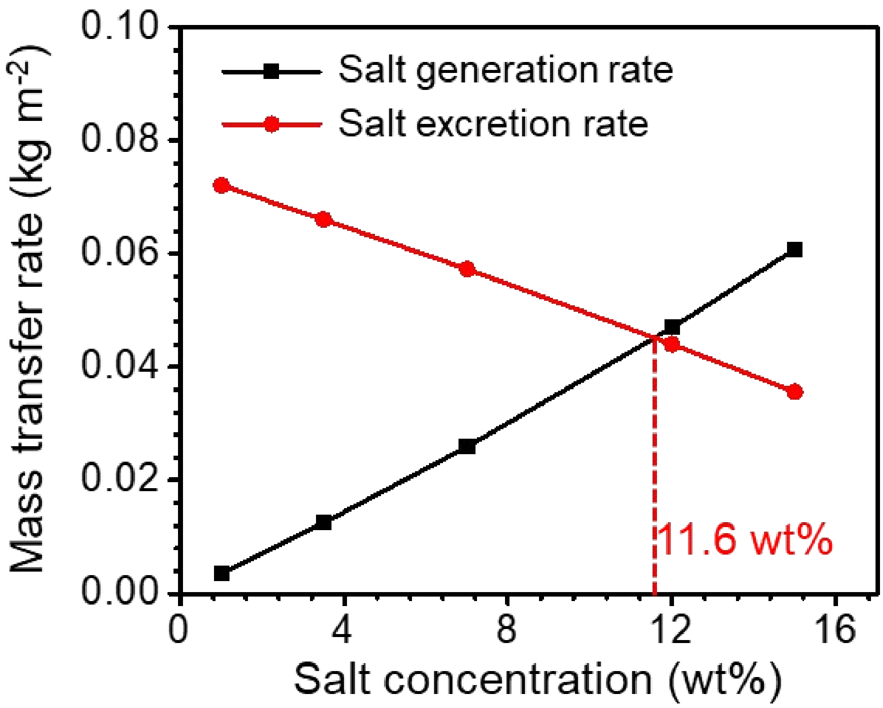

Fig. S9 Concentration dependent salt generation rate and excretion rate in the Janus evaporator under 1-sun irradiance. The salt concentration at the intersection point represents the maximum operation concentration (11.6 wt%) for the Janus evaporator without salt deposition based on the diffusion calculation.

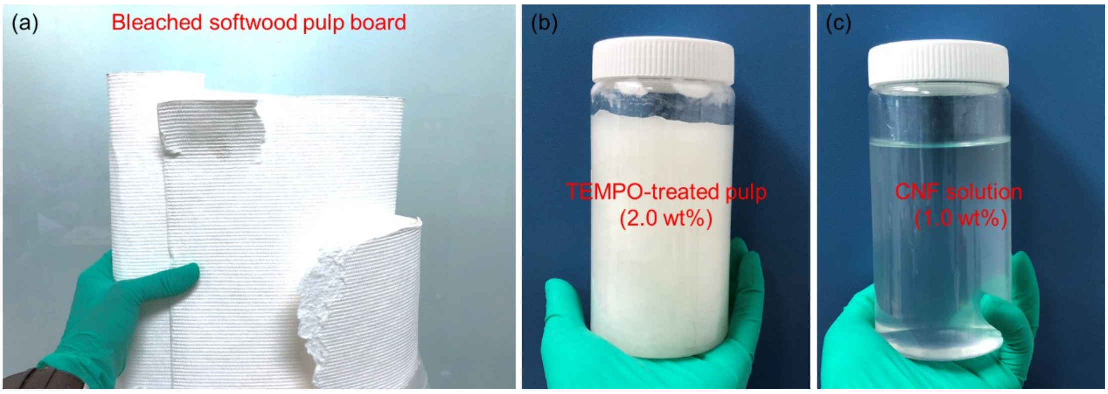

Fig. S10 Photographs illustrating (a) the bleached softwood pulp used for CNF preparation, (b) the 2.0 wt% TEMPO-treated cellulose suspension and (c) the resultant 1.0 wt% CNF solution after homogenization.

Table S1 Steam generation performance of our Janus evaporator compared to other recently reported steam generation devices.

Evaporator	Evaporation rate (kg m^{-2} h^{-1})	Water salinity	Continuous operation time	Reference
Carbonized Bilayer Wood	1.08	0 wt%	1 h	[1]
Plasmonic treated Wood	~0.95	3.6 wt%	8 h	[2]
Wood based biomimetic system	1.27~1.38	3.5 wt%	10 h	[3]
Janus membrane	1~1.15	20 wt%	1 h	[4]
Graphite film	1.01	~23 wt%	20 h	[5]
Graphene/Carbon nanotube based evaporator	1.62	0 wt%	1 h	[6]
Graphene foam	1.4	2.75 wt%	1.5 h	[7]
3D solar evaporator	2.04	0 wt%	~12 h	[8]
Carbon sponge	1.39	0 wt%	3 h	[9]
TiOx-coated stainless steel	0.80	0 wt%	8.5 h	[10]
Wood/CNT	**1.23**	**3.5 wt% ~ 12 wt%**	**100 h**	**Ours**

References

[1] H. Liu, C. Chen, G. Chen, Y. Kuang, X. Zhao, J. Song, C. Jia, X. Xu, E. Hitz, H. Xie, Advanced Energy Materials 2018, 8, 1701616.

[2] M. Zhu, Y. Li, F. Chen, X. Zhu, J. Dai, Y. Li, Z. Yang, X. Yan, J. Song, Y. Wang, Advanced Energy Materials 2018, 8, 1701028.

[3] P.-F. Liu, L. Miao, Z. Deng, J. Zhou, H. Su, L. Sun, S. Tanemura, W. Cao, F. Jiang, L.-D. Zhao, Materials Today Energy 2018, 8, 166.

[4] W. Xu, X. Hu, S. Zhuang, Y. Wang, X. Li, L. Zhou, S. Zhu, J. Zhu, Advanced Energy Materials 2018, 8, 1702884.

[5] S. MohammadáSajadi, S. HiáWang, Journal of Materials Chemistry A 2017, 5, 15227.

[6] X. Hu, W. Xu, L. Zhou, Y. Tan, Y. Wang, S. Zhu, J. Zhu, Advanced Materials 2017, 29,

1604031.

[7] H. Ren, M. Tang, B. Guan, K. Wang, J. Yang, F. Wang, M. Wang, J. Shan, Z. Chen, D. Wei, Advanced Materials 2017, 29, 1702590.

[8] Y. Shi, R. Li, Y. Jin, S. Zhuo, L. Shi, J. Chang, S. Hong, K.-C. Ng, P. Wang, Joule 2018, 2, 1171.

[9] L. Zhu, M. Gao, C. K. N. Peh, X. Wang, G. W. Ho, Advanced Energy Materials 2018, 8, 1702149.

[10] M. Ye, J. Jia, Z. Wu, C. Qian, R. Chen, P. G. O'Brien, W. Sun, Y. Dong, G. A. Ozin, Advanced Energy Materials 2017, 7, 1601811.

Table S2 Properties of the NaCl solution at room temperature which was used for the salt excretion rate calculation.

Weight concentration (wt%)	Volumetric concentration (g l^{-1})	Density (g cm^{-3})
1	10.1	1.005
2	20.3	1.013
3	30.6	1.020
4	41.1	1.027
5	51.7	1.034
6	62.5	1.041
7	73.4	1.049
8	84.5	1.056
9	95.6	1.063
10	107.1	1.071
11	118	1.078
12	130	1.086
13	142	1.093
14	154	1.101
15	166	1.109
16	179	1.116
17	191	1.124
18	204	1.132
19	217	1.140
20	230	1.148
21	243	1.156
22	256	1.164
23	270	1.172
24	283	1.180
25	297	1.189
26	311	1.197
26.4	318	1.200